

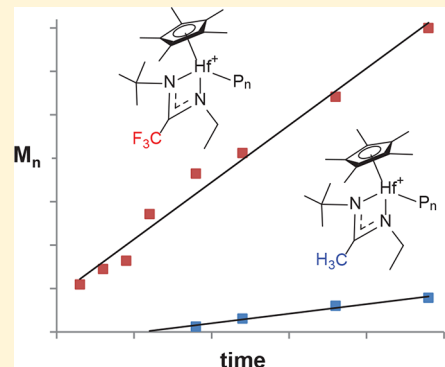
# Electronic Effect Rate Enhancement in the Stereoselective Living Coordinative Polymerization of $\alpha$ -Olefins by $\alpha,\alpha,\alpha$ -Trifluoroacetamidinate-Modified Group 4 Metal CPAM<sup>CF<sub>3</sub></sup> Initiators

Rick R. Thompson, Peter Y. Zavalij, and Lawrence R. Sita\*<sup>ID</sup>

Laboratory of Applied Catalyst Science and Technology, Department of Chemistry and Biochemistry, University of Maryland, College Park, Maryland 20742, United States

 Supporting Information

**ABSTRACT:** The  $C_1$ -symmetric cyclopentadienyl,  $\alpha,\alpha,\alpha$ -trifluoroacetamidinate (CPAM<sup>CF<sub>3</sub></sup>) group 4 metal dimethyl complexes,  $Cp^*[N(Et)C(CF<sub>3</sub>)N('Bu)]M(Me)<sub>2</sub>$  ( $Cp^* = \eta^5-C_5Me_5$ ) for  $M = Zr$  (3) and  $Hf$  (4), serve as initiators for the stereoselective (*isotactic*) living coordination polymerization (LCP) of  $\alpha$ -olefins upon *in situ* “activation” using one equiv of the borate co-initiator,  $[PhNMe_2H][B(C_6F_5)_4]$ . For the LCP of 1-hexene using 4, a six-fold enhancement in the rate of polymerization,  $R_p$ , is observed relative to the LCP of this same  $\alpha$ -olefin when the nonfluorinated CPAM<sup>CH<sub>3</sub></sup> structural analogue,  $Cp^*[N(Et)C(CH<sub>3</sub>)N('Bu)Hf(Me)<sub>2</sub>]$  (2), is employed as the preinitiator. For the LCP of propene, an eight-fold increase in  $R_p$  using the CPAM<sup>CF<sub>3</sub></sup> preinitiator 4 now permits production of practical quantities of highly stereo- and regioregular isotactic polypropene (iPP) under reaction conditions that are not amenable for use with the corresponding CPAM<sup>CH<sub>3</sub></sup> preinitiator 2. These results provide strong support for a unique synergistic coupling of steric and electronic effects of the CPAM<sup>CF<sub>3</sub></sup> ligand environment.



Polyolefins, with a global production volume of over 200 million metric tons per year, easily rank as one of the most important synthetic materials ever devised in terms of the range of technologies and applications currently supported. Nonetheless, the existing profusion of different polyolefin products that are now available can conceivably be expanded upon even further through the design and implementation of new paradigms for olefin polymerization catalysts and reaction processes.<sup>1</sup> Herein, we now report the successful results of an effort to introduce electronic effects associated with the  $\alpha,\alpha,\alpha$ -trifluoroacetamidinate ligand into the known family of cyclopentadienyl, amidinate (CPAM) group 4 metal complexes,  $\{(\eta^5-C_5R_5)[N(R^1)C(X)N(R^2)]M(Me)\}[B]$  ( $M = Zr$  or  $Hf$ ,  $B = [B(C_6F_5)_4]$  or  $[MeB(C_6F_5)_3]$ ) (I), as a means by which to favorably enhance performance as initiators for the stereoselective living coordinative polymerization (LCP) and, by future extension, to the living coordinative chain transfer polymerization (LCCTP) of ethene, propene, higher carbon-numbered  $\alpha$ -olefins, and  $\alpha,\omega$ -nonconjugated dienes.<sup>2,3</sup>

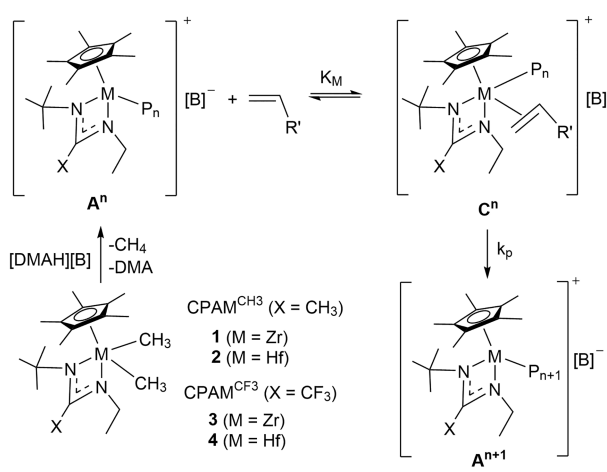
Over the past 20 years, the development and optimization of different derivatives of I for use in the (stereoselective) LCP and LCCTP of olefins has relied exclusively on the manipulation of the magnitude of nonbonded steric interactions between substituents within the CPAM ligand environment that also includes those of the growing polyolefin chain.<sup>2a,c–g,3a,d</sup> For these polymerizations, the ion pair I is generated *in situ* from the corresponding CPAM dimethyl preinitiator,  $(\eta^5-C_5R_5)[N(R^1)C(X)N(R^2)]M(Me)_2$  (II),

through either methyl group protonolysis with the dimethyl-anilinium borate,  $[PhNMe_2(H)][B(C_6F_5)_4]$ , or abstraction by the trityl borate,  $[Ph_3C][B(C_6F_5)_4]$ , or borane,  $B(C_6F_5)_3$ . Surprisingly, however, after all these efforts, to date, the best derivative of II for achieving the highest degree of stereoselectivity in the LCP of  $\alpha$ -olefins still remains the originally reported  $C_1$ -symmetric complexes,  $Cp^*[N(Et)C(Me)N('Bu)]-M(Me)_2$  ( $Cp^* = \eta^5-C_5Me_5$ ) for  $M = Zr$  (1) and  $Hf$  (2), that are shown in Scheme 1. With both of these preinitiators, the LCP of 1-hexene proceeds in a stereospecific and 1,2-regiospecific fashion to provide isotactic poly(1-hexene) (iPH).<sup>2a,f</sup> In the case of propene, 1 and 2 also produce isotactic polypropene (iPP) with a degree of enantiosite selectivity for propagation,  $\alpha$ , of 0.94, which translates into a stereochemical pentad *mmmm* value of 0.71 as established through a <sup>13</sup>C NMR microstructural analysis.<sup>4,5</sup> However, although Zr-based 1 delivers this iPP with up to 3% of 2,1-regioerrors, the corresponding material obtained using the third-row congener 2 is more crystalline and with a higher melting temperature,  $T_m$ , by virtue of propagation now having occurred in a regiospecific manner.<sup>6</sup> Unfortunately, with 2, the observed rate of polymerization,  $R_p$ , of  $\alpha$ -olefins is 60-times slower than that when 1 is employed under otherwise identical conditions,<sup>2f</sup> and it is this Achilles Heel of the Hf-based system

Received: November 15, 2018

Published: December 24, 2018

Scheme 1



that severely limits its utility to provide practical quantities of a desired polyolefin product by LCP.

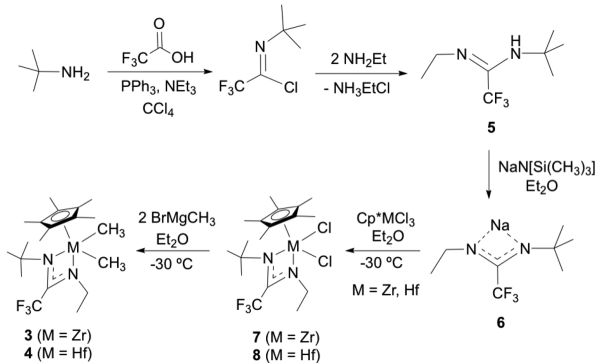
Since further optimization of **I** using steric effects alone had largely reached an impasse, we sought to introduce electronic effects into the CPAM ligand set as a way to gain further polymerization performance in terms of enhanced  $R_p$ , and potentially, higher degrees of stereo- and regioselectivity as well. For this purpose, placement of a formal electron-withdrawing  $CF_3$  group in the distal position of the amidinate ligand seemed to be a reasonable choice based on the simple, but apparently not previously proposed or pursued, hypothesis that an increase in the electrophilicity of the transition-metal center could serve to shift the equilibrium between the active propagating species,  $A^n$ , and the olefin monomer in favor of formation of the  $\pi$ -olefin complex,  $C^n$ , that is required for chain growth propagation through migratory insertion according to Scheme 1.<sup>7–9</sup> On the other hand, an increase in transition-metal electrophilicity could also give rise to “tighter” ion pairing within both **I** and  $A^n$  that manifests as slower rates of initiation and propagation, or in the extreme, no polymerization activity at all.<sup>10</sup> Placement of a  $CF_3$  group within the CPAM ligand environment might also have unintended consequences for the LCP of olefins, both negative and positive, through possible introduction of new metal–fluorine and hydrogen–fluorine secondary bonding interactions.<sup>11</sup> Finally, it is recognized at the outset that the  $CF_3$  group is sterically noninnocent, and, in fact, it has been assessed to be equivalent in size to an isopropyl substituent.<sup>12</sup> Since we have previously shown that both the magnitude of  $R_p$  and degree of stereoselectivity in the LCP of  $\alpha$ -olefins are attenuated by an increase in the steric bulk of the distal X-substituent of the amidinate ligand in **I**,<sup>2e</sup> it is conceivable that the proposed strategy based on Scheme 1 could potentially backfire and actually lead to a less desirable overall polymerization performance.

In practice, the main challenge initially encountered in pursuing an experimental validation of our new strategy with  $CPAM^{CF_3}$  derivatives of **I** and **II** ( $X = CF_3$ ) was the absence in the literature of any report whatsoever detailing the synthesis and characterization of lanthanide, transition-metal, or main-group metal complexes supported by an  $\alpha,\alpha,\alpha$ -trifluoroacetamidinate ligand, and this includes examples of alkali metal

$\alpha,\alpha,\alpha$ -trifluoroacetamidinate salts,  $[N(R^1)C(CF_3)N(R^2)][M]$  (where  $M = Li$ ,  $Na$ , or  $K$ ), that could potentially serve as key reagents.<sup>13</sup> Indeed, in the only report of an  $\alpha,\alpha,\alpha$ -trifluoroacetamidine transition-metal complex, the sterically encumbered amidine ligand,  $N(H)(Ar)C(CF_3)N(Ar)$  [ $Ar = 2,6-(iPr)_2C_6H_3$ ], is actually coordinated in  $\eta^6$ -arene fashion to a  $Mo(CO)_3$  fragment rather than through metal–nitrogen bonds.<sup>14</sup> Finally, this literature survey revealed that, in general, synthetic methods that can be used to access a range of symmetric and unsymmetric  $\alpha,\alpha,\alpha$ -trifluororoacetamidines,  $N(H)(R^1)C(CF_3)N(R^2)$ , have remained largely undeveloped.<sup>15</sup>

Scheme 2 summarizes the synthetic routes used in the present work to prepare the desired new  $CPAM^{CF_3}$

Scheme 2



preinitiators,  $Cp^*[N(^3Bu)C(CF_3)N(Et)]M(Me)_2$  for  $M = Zr$  (**3**) and  $Hf$  (**4**).<sup>16</sup> To begin, synthesis of the unsymmetric  $CF_3$ -amidine,  $[N(^3Bu)C(CF_3)N(H)(Et)]$  (**5**), was achieved through a two-step procedure involving a trifluoroacetimidoyl chloride intermediate according to the procedure of Uneyama and co-workers.<sup>15</sup> Deprotonation of **5** was then accomplished through addition of a slight stoichiometric excess of sodium hexamethyldisilazide,  $[NaN(SiMe_3)_2]$ , to a diethyl ether ( $Et_2O$ ) solution to provide the etherate complex,  $[N(^3Bu)C(CF_3)N(Et)][Na(OEt_2)]$  (**6**), as an analytically pure, dark-red crystalline material after removal of the volatiles and recrystallization of the crude material from pentane at  $-30$   $^{\circ}C$ .<sup>16</sup> A single-crystal X-ray analysis of **6** revealed the polymeric solid-state structure shown in Figure 1a that is composed of a linear chain of amidinate units that are connected through a repeating intermolecular  $Na1-N1$  bond of  $2.420(2)$   $\text{\AA}$ . Additional intramolecular  $Na1-N2$ ,  $Na1-F3$ , and  $Na1-O1$  bonding interactions of  $2.383(2)$   $\text{\AA}$ ,  $2.362(17)$   $\text{\AA}$ , and  $2.374(2)$   $\text{\AA}$ , respectively, complete the coordination sphere about the  $Na$  cation.

As Scheme 2 further presents, synthesis of the required  $CPAM^{CF_3}$  second- and third-row group 4 metal dichlorides,  $Cp^*[N(^3Bu)C(CF_3)N(Et)]M(Cl)_2$ , where  $M = Zr$  (**7**) and  $Hf$  (**8**), was accomplished through addition of a stoichiometric equivalent of *in situ*-generated **6** to the corresponding  $Cp^*MCl_3$  starting materials in  $Et_2O$ .<sup>16</sup> Both **7** and **8** were isolated as crystalline materials, and X-ray crystallography served to confirm that the  $CF_3$ -amidine ligand coordinates to the group 4 metal in a  $\kappa-N,N'$ -bidentate fashion. This solid-state molecular structure of **8** is shown in Figure 1b, while that for **7** is presented in the Supporting Information. These data also provide the opportunity to assess the magnitude of the steric impact that the distal  $CF_3$  group has on the overall

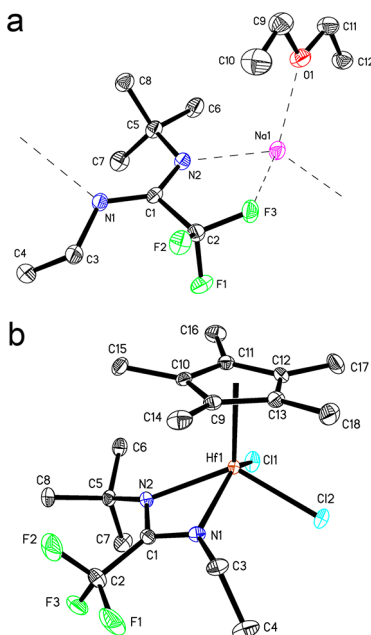


**Figure 1.** Molecular structures (30% thermal ellipsoids) of (a) 6 and (b) 8. Hydrogen atoms have been removed for the sake of clarity.

CPAM<sup>CF<sub>3</sub></sup> ligand sphere about the transition-metal center. For this purpose, **Table 1** presents selected bond angles for 7 and 8

**Table 1. Selected Bond Angles for**  
**Cp\*[N('Bu)C(X)N(Et)]M(Y)<sub>2</sub>**

X, M, Y	M–N–C <sub>tBu</sub> (deg)	M–N–C <sub>Et</sub> (deg)
tBu, Zr, Cl	136.6(2)	131.4(2)
CF <sub>3</sub> , Zr, Cl (7)	137.10(7)	133.33(8)
CF <sub>3</sub> , Hf, Cl (8)	137.5(1)	133.3(1)
Ph, Zr, Cl	140.6(2)	140.4(2)
H, Zr, Cl	146.40(9)	145.64(16)
tBu, Zr, CH <sub>3</sub>	135.1(3)	132.7(3)
CH <sub>3</sub> , Hf, CH <sub>3</sub>	139.9(3)	138.6(3)
CH <sub>3</sub> , Zr, CH <sub>3</sub>	142.5(16)	136.4(17)
H, Zr, CH <sub>3</sub>	147.30(7)	141.20(8)

along with corresponding values for a series of closely related CPAM<sup>X</sup> group 4 metal dichloride and dimethyl analogues.<sup>2,3</sup> As can be seen, the M–N–C<sub>tBu</sub> and M–N–C<sub>Et</sub> bond angles are highly sensitive to the magnitude of “buttressing” interactions between the distal X substituent and the N-<sup>t</sup>Bu and N-ethyl groups of the amidinate ligand that help to define the extent of steric crowding about the transition-metal center. Of significant importance to the current study is the observation that the distal CF<sub>3</sub> group of 7 and 8 appears to have a steric impact within the CPAM ligand sphere that lies somewhere between those manifested by distal Ph and <sup>t</sup>Bu groups and is significantly larger than that of distal CH<sub>3</sub> and H substituents.

As a final synthetic consideration, **Scheme 2** confirms that the desired group 4 CPAM<sup>CF<sub>3</sub></sup> dimethyl preinitiators, 3 and 4, could be prepared through methylation of 7 and 8, respectively, using two equivalents of methyl magnesium bromide. Unfortunately, unlike their dichloride precursors, both 3 and 4 were found to exist as very viscous, yellow oils

that tend to retain solvent tightly, and as such, confirmation of molecular structure could not be unequivocally confirmed by X-ray crystallography, nor was it possible to obtain a satisfactory elemental analysis in each case. On the other hand, a high degree of chemical purity (>95%) was established for both 3 and 4 through <sup>1</sup>H, <sup>13</sup>C, and <sup>19</sup>F NMR spectroscopy.<sup>16</sup> Interestingly, <sup>1</sup>H NMR (400 MHz, benzene-d<sub>6</sub>, 25 °C) spectra of both 3 and 4 display a well-defined long-range <sup>5</sup>J(<sup>1</sup>H–<sup>19</sup>F) coupling constant of 2.4 Hz between the distal CF<sub>3</sub> group and the methylene (CH<sub>2</sub>) unit of the N-Et substituent. Furthermore, in keeping with other derivatives of I, only a single <sup>1</sup>H resonance is observed for the two diastereotopic M-Me groups in the <sup>1</sup>H NMR spectra of 3 and 4, and a preliminary variable-temperature <sup>1</sup>H NMR investigation of the latter confirmed that rapid metal-centered racemization occurs through an intramolecular “amidinate ring-flipping” process that has an associated free energy of activation,  $\Delta G^\ddagger$ , of <10 kcal mol<sup>-1</sup> at the coalescence temperature,  $T_c$ , of 243 K according to an Eyring analysis. Surprisingly, this  $\Delta G^\ddagger$  value for the CPAM<sup>CF<sub>3</sub></sup> derivative 4 closely matches in magnitude that established for the CPAM<sup>CH<sub>3</sub></sup> analogue 2.<sup>2a</sup>

As further proof of structure and composition, both 3 and 4 indeed proved capable of serving as preinitiators for the stereoselective LCP of 1-hexene and propene. However, because of the higher level of spectroscopically confirmed purity that could be routinely obtained for 4, the preliminary LCP studies reported herein were performed using this CPAM<sup>CF<sub>3</sub></sup> preinitiator. Thus, addition of 200 equiv of 1-hexene to the clear yellow “initiator” solution formed from prior addition of 1 equiv of [PhNMe<sub>2</sub>H][B(C<sub>6</sub>F<sub>4</sub>)<sub>4</sub>] to 4 in chlorobenzene (PhCl) at -10 °C, provided an excellent yield of iPH after a 10 h polymerization time and the usual workup.<sup>16</sup> Analytical characterization of this iPH material by gel permeation chromatography (GPC) gave number-average and weight-average molecular weight indices,  $M_n$  and  $M_w$ , of 18.2 kDa and 18.5 kDa, respectively, which together establish a polydispersity  $D$  value of 1.02. A <sup>1</sup>H NMR (800 MHz, 1,1,2,2-CD<sub>2</sub>Cl<sub>4</sub>, 90 °C) spectrum of this iPH further showed the absence of resonances for vinyl end-groups that might arise through chain termination via  $\beta$ -hydrogen transfer processes. Finally, a <sup>13</sup>C{<sup>1</sup>H} NMR (200 MHz) stereochemical microstructure analysis of this same sample confirmed that chain growth propagation had occurred in a strict stereoselective and 1,2-regiospecific manner. Collectively, these results provide overwhelming evidence for quantitative formation of the desired Hf-based CPAM<sup>CF<sub>3</sub></sup> initiator from 4 and its ability to effect the stereospecific and regiospecific LCP of 1-hexene. Most importantly, however, a kinetic analysis not only established the expected linear relationship between  $M_n$  and time, but also that the observed  $R_p$  for this 1-hexene polymerization using the CPAM<sup>CF<sub>3</sub></sup> preinitiator 4 was six-times larger than that obtained using the corresponding CPAM<sup>CH<sub>3</sub></sup> preinitiator 2. Finally, the LCP of propene using 4 was also conducted, and under our standard conditions, a more than eight-fold increase in the observed rate of polymerization could now be realized [cf. iPP from 2:  $M_n$  = 6.2 kDa ( $D$  = 1.63) vs from 4:  $M_n$  = 49.9 kDa ( $D$  = 1.62)].<sup>6</sup> Importantly, this higher  $R_p$  value for the Hf-based CPAM<sup>CF<sub>3</sub></sup> system based on 4 is achieved without a sacrifice in either the degree of stereo- or regiospecificity previously provided by 2, and on a practical level, this means that the former can now be used to access a higher targeted molecular weight for the polyolefin product

within a more reasonable polymerization time than that previously possible with the latter.

Although the exact origin of the electronic effects introduced by the  $\alpha,\alpha,\alpha$ -trifluoroacetamidinate ligand into the CPAM family of initiators for the LCP and LCCTP of olefins still remains to be more firmly established through additional experimental studies and computational modeling, it is clear that these can operate in a synergistic fashion with previously established substituent-based steric effects. Efforts are now in progress to further develop the CPAM<sup>CF<sub>3</sub></sup> ligand set for both living and nonliving olefin polymerization catalysts.

## ■ ASSOCIATED CONTENT

### § Supporting Information

The Supporting Information is available free of charge on the ACS Publications website at DOI: [10.1021/acs.organomet.8b00839](https://doi.org/10.1021/acs.organomet.8b00839).

Experimental details, supporting figures (PDF)

### Accession Codes

CCDC 1869268–1869270 contain the supplementary crystallographic data for this paper. These data can be obtained free of charge via [www.ccdc.cam.ac.uk/data\\_request/cif](http://www.ccdc.cam.ac.uk/data_request/cif), or by emailing [data\\_request@ccdc.cam.ac.uk](mailto:data_request@ccdc.cam.ac.uk), or by contacting The Cambridge Crystallographic Data Centre, 12 Union Road, Cambridge CB2 1EZ, UK; fax: +44 1223 336033.

## ■ AUTHOR INFORMATION

### Corresponding Author

\*E-mail: [lsita@umd.edu](mailto:lsita@umd.edu).

### ORCID

Lawrence R. Sita: [0000-0002-9880-1126](https://orcid.org/0000-0002-9880-1126)

### Notes

The authors declare no competing financial interest.

## ■ ACKNOWLEDGMENTS

We thank the National Science Foundation (CHE-1665421) for financial support of this work.

## ■ REFERENCES

- (1) See, for example: (a) Domski, G. J.; Rose, J. M.; Coates, G. W.; Bolig, A. D.; Brookhart, M. Living Alkene Polymerization: New Methods for the Precision Synthesis of Polyolefins. *Prog. Polym. Sci.* **2007**, *32*, 30–92. (b) Wenzel, T. T.; Arriola, D. J.; Carnahan, E. M.; Hustad, P. D.; Kuhlman, R. L. Chain Shuttling Catalysis and Olefin Block Copolymers (OBCs). *Top. Organomet. Chem.* **2009**, *26*, 65–104. (c) Sita, L. R. Ex Uno Plures (“Out of One, Many”): New Paradigms for Expanding the Range of Polyolefins through Reversible Group Transfers. *Angew. Chem., Int. Ed.* **2009**, *48*, 2464–2472. (d) Valente, A.; Mortreux, A.; Visseaux, M.; Zinck, P. Coordinative Chain Transfer Polymerization. *Chem. Rev.* **2013**, *113*, 3836–3857. (e) Sturzel, M.; Mihan, S.; Mulhaupt, R. From Multisite Polymerization Catalysis to Sustainable Materials and All-Polyolefin Composites. *Chem. Rev.* **2016**, *116*, 1398–1433. (f) Chen, C. Designing Catalysts for Olefin Polymerization and Copolymerization: Beyond Electronic and Steric Tuning. *Nature. Rev. Chem.* **2018**, *2*, 6–14.
- (2) For LCP using group 4 metal CPAM initiators, see: (a) Jayaratne, K. C.; Sita, L. R. Stereospecific Living Ziegler-Natta Polymerization of 1-Hexene. *J. Am. Chem. Soc.* **2000**, *122*, 958–959. (b) Jayaratne, K. C.; Keaton, R. J.; Henningsen, D. A.; Sita, L. R. Living Ziegler-Natta Cyclopolymerization of Nonconjugated Dienes: New Classes of Microphase-separated Polyolefin Block Copolymers. *J. Am. Chem. Soc.* **2000**, *122*, 10490–10491. (c) Keaton, R. J.; Jayaratne, K. C.; Henningsen, D. A.; Koterwas, L. A.; Sita, L. R. Dramatic Enhancement of Activities for Living Ziegler-Natta Polymerization Mediated by Exposed Zirconium Acetamidinate Initiators: The Isospecific Living Polymerization of Vinylcyclohexene. *J. Am. Chem. Soc.* **2001**, *123*, 6197–6198. (d) Kissounko, D. A.; Fettinger, J. C.; Sita, L. R. Structure/Activity Relationships for the Living Ziegler-Natta Polymerization of 1-Hexene by the Series of Cationic Monocyclopentadienyl Zirconium Acetamidinate Complexes, [( $\eta^5$ -C<sub>5</sub>Me<sub>5</sub>)ZrMe{N(CH<sub>2</sub>R)C(Me)N(t-Bu)}][B(C<sub>6</sub>F<sub>5</sub>)<sub>4</sub>] (R = Me, i-Pr, t-Bu, Ph, 2-ClC<sub>6</sub>H<sub>4</sub>, 3-MeC<sub>6</sub>H<sub>4</sub>, and 2,4,6-Me<sub>3</sub>C<sub>6</sub>H<sub>2</sub>). *Inorg. Chim. Acta* **2003**, *345*, 121–129. (e) Zhang, Y.; Reeder, E. K.; Keaton, R. J.; Sita, L. R. Goldilocks Effect of a Distal Substituent on Living Ziegler-Natta Polymerization Activity and Stereoselectivity within a Class of Zirconium Amidinate-Based Initiators. *Organometallics* **2004**, *23*, 3512–3520. (f) Kissounko, D. A.; Zhang, Y.; Harney, M. B.; Sita, L. R. Evaluation of [( $\eta^5$ -C<sub>5</sub>Me<sub>5</sub>)Hf(R)<sub>2</sub>[N(Et)C(Me)N(t-Bu)]] (R = Me and i-Bu) for the Stereospecific Living and Degenerative Transfer Living Ziegler-Natta Polymerization of  $\alpha$ -Olefins. *Adv. Synth. Catal.* **2005**, *347*, 426–432. (g) Zhang, W.; Sita, L. R. Investigation of Dynamic Intra- and Intermolecular Processes within a Tether-length Dependent Series of Group 4 Bimetallic Initiators for Stereo-modulated Degenerative Transfer Living Ziegler-Natta Propene Polymerization. *Adv. Synth. Catal.* **2008**, *350*, 439–447. (h) Crawford, K. E.; Sita, L. R. Stereoengineering of Poly(1,3-methylenecyclohexane) via Two-State Living Coordination Polymerization of 1,6-Heptadiene. *J. Am. Chem. Soc.* **2013**, *135*, 8778–8781.
- (3) For LCCTP using group 4 metal CPAM initiators, see: (a) Zhang, W.; Sita, L. R. Highly Efficient, Living Coordinative Chain-Transfer Polymerization of Propene with ZnEt<sub>2</sub>: Practical Production of Ultrahigh to Very Low Molecular Weight Atactic Polypropene of Extremely Narrow Polydispersity. *J. Am. Chem. Soc.* **2008**, *130*, 442–443. (b) Zhang, W.; Wei, J.; Sita, L. R. Living Coordinative Chain Transfer Polymerization and Copolymerization of Ethene,  $\alpha$ -Olefins and  $\alpha,\omega$ -Nonconjugated Dienes using Dialkylzinc as Surrogate Chain-growth Sites. *Macromolecules* **2008**, *41*, 7829–7833. (c) Wei, J.; Zhang, W.; Sita, L. R. *Angew. Chem., Int. Ed.* **2010**, *49*, 1768–1772. (d) Wei, J.; Zhang, W.; Wickham, R.; Sita, L. R. Programmable Modulation of Co-monomer Relative Reactivities for Living Coordination Polymerization through Reversible Chain Transfer between Tight and Loose Ion Pairs. *Angew. Chem., Int. Ed.* **2010**, *49*, 9140–9144. (e) Wei, J.; Hwang, W.; Zhang, W.; Sita, L. R. Dinuclear Bis-Propagators for the Stereospecific Living Coordinative Chain Transfer Polymerization of Propene. *J. Am. Chem. Soc.* **2013**, *135*, 2132–2135. (f) Thomas, T. S.; Hwang, W.; Sita, L. R. End-Group Functionalized Poly( $\alpha$ -olefines) as Non-polar Building Blocks: Self-Assembly of Sugar-Polyolefin Hybrid Conjugates. *Angew. Chem., Int. Ed.* **2016**, *55*, 4683–4687.
- (4) Harney, M. B.; Zhang, Y.; Sita, L. R. Bimolecular Control Over Polypropene Stereochemical Microstructure in a Well-Defined Two-state System and a New Fundamental Form: Stereogradient Polypropene. *Angew. Chem., Int. Ed.* **2006**, *45*, 6140–6144.
- (5) Busico, V.; Cipullo, R. Microstructure of Polypropene. *Prog. Polym. Sci.* **2001**, *26*, 443–533.
- (6) Although no chain termination is evident for the LCP of either olefin by Hf-based CPAM initiators, a larger molecular weight distribution is observed for iPP relative to iPH (cf.  $D$  (=M<sub>w</sub>/M<sub>n</sub>) of 1.62 vs 1.02, respectively). The origin of this difference is currently under investigation.
- (7) (a) Cossee, P. Ziegler-Natta Catalysis. I. Mechanism of Polymerization of  $\alpha$ -Olefins with Ziegler-Natta Catalysts. *J. Catal.* **1964**, *3*, 80–88. (b) Arlman, E. J.; Cossee, P. Ziegler-Natta Catalysis. III. Stereospecific Polymerization of Propene with the Catalyst System TiCl<sub>3</sub>-AlEt<sub>3</sub>. *J. Catal.* **1964**, *3*, 99–104. (c) Doi, Y.; Ueki, S.; Keii, T. Living Coordination Polymerization of Propene Initiated by the Soluble Tris(acetylacetonato)vanadium-chlorodiethylaluminum system. *Macromolecules* **1979**, *12*, 814–819. (d) Doi, Y.; Takada, M.; Keii, T. Molecular Weight Distribution and Kinetics of Low-Temperature Propene Polymerization with Soluble Vanadium-based Ziegler Catalysts. *Bull. Chem. Soc. Jpn.* **1979**, *52*, 1802–1806.

(e) Deng, L.; Ziegler, T.; Woo, T. K.; Margl, P.; Fan, L. Computer Design of Living Olefin Polymerization Catalysts: A Combined Density Functional Theory and Molecular Mechanics Study. *Organometallics* **1998**, *17*, 3240–3253. (f) Ajjou, J. A. N.; Scott, S. L. A Kinetic Study of Ethylene and 1-Hexene Homo- and Copolymerization Catalyzed by a Silica-Supported Cr(IV) Complex: Evidence for Propagation by a Migratory Insertion Mechanism. *J. Am. Chem. Soc.* **2000**, *122*, 8968–8976. (g) Ciancaleoni, G.; Fraldi, N.; Budzelaar, P. H. M.; Busico, V.; Cipullo, R.; Macchioni, A. Structure-Activity Relationship in Olefin Polymerization Catalysis: Is Entropy the Key? *J. Am. Chem. Soc.* **2010**, *132*, 13651–13653. (h) Ehm, C.; Budzelaar, P. H. M.; Busico, V. Tuning the Relative Energies of Propagation and Chain Termination Barriers in Polyolefin Catalysis through Electronic and Steric Effects. *Eur. J. Inorg. Chem.* **2017**, *2017*, 3343–3349.

(8) Margl, P.; Deng, L.; Ziegler, T. A Unified View of Ethylene Polymerization by d(0) and d(0)f(n) Transition Metals. 1. Precursor Compounds and Olefin Uptake Energetics. *Organometallics* **1998**, *17*, 933–946.

(9) According to the mechanism of [Scheme 1](#),

$$R_p = k_p \left[ \frac{K_m[M]}{1 + K_m[M]} \right] [A^n]$$

where M is monomer and A<sup>n</sup> is propagator.

(10) (a) Piccolrovazzi, N.; Pino, P.; Consiglio, G.; Sironi, A.; Moret, M. Electronic Effects in Homogeneous Indenylzirconium Ziegler-Natta Catalysts. *Organometallics* **1990**, *9*, 3098–3105. (b) Lee, I.-M.; Gauthier, W. J.; Ball, J. M.; Iyengar, B.; Collins, S. Electronic Effects of Ziegler-Natta Polymerization of Propylene and Ethylene Using Soluble Metallocene Catalysts. *Organometallics* **1992**, *11*, 2115–2122. (c) Thornberry, M. P.; Reynolds, N. T.; Deck, P. A.; Fronczeck, F. R.; Rheingold, A. L.; Liable-Sands, L. M. Synthesis, Structure, and Olefin Polymerization Catalytic Behavior of Aryl-Substituted Zirconocene Dichlorides. *Organometallics* **2004**, *23*, 1333–1339. (d) Popeney, C.; Guan, Z. Ligand Electronic Effects on Late Transition Metal Polymerization Catalysts. *Organometallics* **2005**, *24*, 1145–1155. (e) Song, D.; Shi, X.; Wang, Y.; Yang, J.; Li, Y. Ligand Steric and Electronic Effects on  $\beta$ -Ketiminato Neutral Nickel(II) Olefin Polymerization Catalysts. *Organometallics* **2012**, *31*, 966–975. (f) Nifant'ev, I. E.; Ivchenko, P. V.; Bagrov, V. V.; Churakov, A. V.; Mercandelli, P. 5-Methoxy-substituted Zirconium Bis-indenyl Ansa-complexes: Synthesis, Structure and Catalytic Activity in the Polymerization and Copolymerization of Alkenes. *Organometallics* **2012**, *31*, 4962–4970. (g) Elkin, T.; Aharonovich, S.; Botoshansky, M.; Eisen, M. S. Synthesis and Characterization of Group 4 Fluorinated Bis(amidinates) and Their Reactivity in the Formation of Elastomeric Polypropylene. *Organometallics* **2012**, *31*, 7404–7414. (h) Wang, J.; Yao, E.; Chen, Z.; Ma, Y. Fluorinated Nickel(II) Phenoxyiminato Catalysts: Exploring the Role of Fluorine Atoms in Controlling Polyethylene Productivities and Microstructure. *Macromolecules* **2015**, *48*, 5504–5510.

(11) (a) Saito, J.; Mitani, M.; Mohri, J.; Ishii, S.; Yoshida, Y.; Matsugi, T.; Kojoh, S.; Kashiwa, N.; Fujita, T. Highly Syndiospecific Living Polymerization of Propylene Using a Titanium Complex Having Two Phenoxy-imine Chelate Ligands. *Chem. Lett.* **2001**, *30*, 576–577. (b) Tian, J.; Hustad, P. D.; Coates, G. W. A New Catalyst for Highly Syndiospecific Living Olefin Polymerization: Homopolymers and Block Copolymers from Ethylene and Propylene. *J. Am. Chem. Soc.* **2001**, *123*, 5134–5135. (c) Zuideveld, M. A.; Wehrmann, P.; Röhr, C.; Mecking, S. Remote Substituents Controlling Catalytic Polymerization by Very Active and Robusts Neutral Nickel(II) Complexes. *Angew. Chem., Int. Ed.* **2004**, *43*, 869–873. (d) Goettker-Schnetmann, I.; Wehrmann, P.; Roehr, C.; Mecking, S. Substituent Effects in ( $\kappa^2$ -N,O)-Salicylaldiminato Nickel(II)-methyl Pyridine Polymerization Catalysts: Terphenyls Controlling Polyethylene Microstructure. *Organometallics* **2007**, *26*, 2348–2362. (e) Weberski, M. P.; Chen, C.; Delferro, M.; Zuccaccia, C.; Macchioni, A.; Marks, T. J. Suppression of  $\beta$ -Hydride Chain Transfer

in Nickel(II)-Catalyzed Ethylene Polymerization via Weak Fluorocarbon Ligand-Product Interactions. *Organometallics* **2012**, *31*, 3773–3789. (f) Iwashita, A.; Chan, M. C. W.; Makio, H.; Fujita, T. Attractive Interactions in Olefin Polymerization Mediated by Post-metallocene Catalysts with Fluorine-Containing Ancillary Ligands. *Catal. Sci. Technol.* **2014**, *4*, 599–610. (g) Liu, C.; Chan, M. C. W. Chelating  $\sigma$ -Aryl Post-metallocenes: Probing Intramolecular [C–H F–C] Interactions and Unusual Reaction Pathways. *Acc. Chem. Res.* **2015**, *48*, 1580–1590.

(12) Belot, V.; Farran, D.; Jean, M.; Albalat, M.; Vanthuyne, N.; Roussel, C. Steric Scale of Common Substituents from Rotational Barriers of N-(*o*-Substituted aryl)thiazoline-2-thione Atropisomers. *J. Org. Chem.* **2017**, *82*, 10188–10200.

(13) (a) Barker, J.; Kilner, M. The Coordination Chemistry of the Amidine Ligand. *Coord. Chem. Rev.* **1994**, *133*, 219–300. (b) Edelmann, F. T. Lanthanide Amidinates and Guanidinates in Catalysis and Materials Science: A Continuing Success Story. *Chem. Soc. Rev.* **2012**, *41*, 7657–7672. (c) Edelmann, F. T. Recent Progress in the Chemistry of Metal Amidinates and Guanidinates: Syntheses, Catalysis and Materials. *Adv. Organomet. Chem.* **2013**, *61*, 55–374.

(14) Boeré, R. T.; Klassen, V.; Wolmershäuser, G. Superamidines 2. Synthesis of the Bulky Ligand N,N-bis-(2,6-diisopropylphenyl)-trifluoroacetamidine and Its Molybdenum Carbonyl Complex. *Can. J. Chem.* **2000**, *78*, 583–589.

(15) Tamura, K.; Mizukami, H.; Maeda, K.; Watanabe, H.; Uneyama, K. One-pot Synthesis of Trifluoroacetimidoyl Halides. *J. Org. Chem.* **1993**, *58*, 32–35.

(16) Details are provided in the [Supporting Information](#).